Silicon (2022) 14:10081–10086
https://doi.org/10.1007/s12633-022-01732-5

ORIGINAL PAPER

# The Effect of Oxidation Temperature on the (1000–1300) $cm^{-1}$ Band in FT-IR Spectra of Silicon Oxide Synthesized by Thermal Oxidation of Silicon Wafers

**Kamal Kayed**[1] · **Dalal Baba Kurd**[1]

Received: 4 September 2021 / Accepted: 31 January 2022 / Published online: 18 February 2022


**Abstract**
In this work, silicon wafers were thermal treated in air at temperatures varied in the range 800—1200 °C. The annealed samples were investigated using FTIR, X-ray diffraction, FTIR and optical reflection spectroscopy. The effect of annealing temperature on the (1000–1300) $cm^{-1}$ band in FT-IR spectra of the prepared samples was investigated. The results showed that thermal oxidation at temperatures less than 1200 °C leads to enhance the phenomenon of the splitting of longitudinal optical and transverse optical stretching motions. This phenomenon was verified by observing the appearance of two overlapping peaks in the region (1000–1300) $cm^{-1}$ in FT-IR spectra. The results also showed that the splitting process leads to the formation of defects in the crystal structure of silicon, which in turn leads to the formation of silicon nanoparticles.

**Keywords** Silicon · Amorphous silicon oxide · FTIR · XRD · Oxidation · Silicon nanoparticles · FTIR · Longitudinal optical motions · Transverse optical stretching motions

## 1 Introduction

The oxidation of silicon surfaces shows promising properties that have made them the focus of many research groups [1–18], which have sought to employ various silicon oxidation techniques in the fabrication of semiconductor devices. These oxidized layers can be used as a key ingredient in creating many electronic devices such as, passivated contacts in silicon solar cells [1, 2], multi-junction quantum well solar cells [7, 8], and barrier layer in silicon-based single and passivation of the amorphous/crystalline Si (a-Si:H/c-Si) heterojunction [4–6], etc.

Thermal oxidation of silicon wafers occurs according to two different mechanisms. At high oxygen gas pressures and low temperature $SiO_2$ layer growth takes place (passive oxidation) according to the reaction $Si + O_2 \rightarrow SiO_2$ [17]. This oxidation method is suitable for industrial applications. In the case of low oxygen gas pressures and high temperature, SiO is desorbed in an etching process (active oxidation) according to the reaction $2Si + O_2 \rightarrow 2SiO$. In this case, the silicon surface remains free of oxide [17] with the possibility of formation of volatile SiO because of high temperature $SiO_2$/Si decomposition via the apparent reaction $Si + SiO_2 \rightarrow 2SiO$ when the oxygen pressure is low. On the other hand, the reoxidation reaction is also possible [17]. Silicon oxide decomposition can be used to help obtain a clean silicon surface [19], but at the same time, the electrical properties of silicon can be damaged because of this process. In fact, passive oxidation (formation of $SiO_2$), active oxidation (formation of SiO (gas)) and $SiO_2$ decomposition are considered separately, with the exception of the transition regime and the first monolayer stage of passive oxidation where these reactions are competitive. The transport of the silicon monoxide (SiO) into gas phase has been noticed only during active oxidation and oxide decomposition processes in vacuum [17]. The processes of decomposition and transition to the gas phase are important factors in determining the growth mechanism of silicon oxide layers.

In silicon oxide layers, silicon nanostructures may be present in the silicon oxide matrix. The, nucleation of Si nanoparticles is induced by a high temperature during the oxidation process. Depending on the deposition conditions and on the temperature and duration of the annealing processes, it is possible to obtain crystalline or amorphous aggregates

✉ Kamal Kayed
khmk2000@gmail.com

[1] Department of Physics, Faculty of Science, Damascus University, Damascus, Syria

Si-nc with different sizes and distributions embedded into a SiO*x* matrix [20]. The presence of such nanoformations in the structure of silicon oxide greatly influences its overall electrical and optical properties.

In our previous work [21], we got important results include the possibility of using the thermal oxidation of silicon in air to obtain $Si/SiO_x$ composites with controllable optical properties suitable for application in the field of semiconductor device synthesis. On the other hand, we found that, the phenomena of splitting of transverse optical stretching and longitudinal optical vibrations effect on the optical absorption coefficient. In addition, we found that, the intensity of the XRD silicon peak is proportional to the relative absorption coefficient of amorphous $SiO_x$. Our present work is continuation of our previous work [21]. Here, we attempt to probe the possible effects of the phenomenon of the splitting of longitudinal optical and transverse optical stretching motions (observed in the infrared spectra of silicon oxide) on the optical and structural properties of the $Si/SiO_x$ composites.

## 2 Experimental

### 2.1 Sample Preparation

In order to prepare layers of silicon oxide on silicon substrates we subjected thoroughly cleaned Pure n-type Si(111) wafers (99.99%) to thermal oxidation in air using a suitable furnace. This process leads to the surface oxidation of the silicon wafers, thus obtaining oxidized surface layers (thin films). Table 1 contains the thermal treatment conditions for each sample.

### 2.2 Sample Characterization

The chemical composition of the samples was examined by using a FTIR spectrophotometer (JASCO- 4200) in the range 400–1300 $cm^{-1}$, with resolutions of 4 $cm^{-1}$. The crystallite structure of the films was measured by X-ray diffraction (XRD) using Philips Analytical X-Ray diffractometer employing a Cu $K\alpha_1$ ($\lambda = 1.54060$ Å) source. The optical reflection spectra were recorded with a UV–Vis spectrophotometer (Cary 5000).

**Table 1** The thermal treatment conditions for each sample

| Sample name | Temperature | Thermal processing time |
|---|---|---|
| A | – | – |
| B | 800°C | 4 h |
| C | 900°C | 4 h |
| D | 1000°C | 4 h |
| E | 1100°C | 4 h |
| F | 1200°C | 4 h |

## 3 Results and Discussion

X-ray diffraction measurements were carried out on all prepared samples. The spectra did not show any characteristic Bragg peaks for silicon oxide, indicating the amorphous structure of this oxide. Figure 1 contains a sample of the XRD spectra that we obtained, which is related to the sample annealed at 1200 °C (sample F). In all measured XRD spectra, the sharp peak is related to Si (111) (CSM card no. 65–1060).

Figure 2 shows the (1000–1300) $cm^{-1}$ band in FT-IR spectra of the prepared samples (detailed characterization of the spectra was covered in a previous work [21]). This broad and intense band is attributed to asymmetric and symmetric stretching vibrations of Si–O-Si bonds [20]. The shoulder at 1190 $cm^{-1}$ appears due to the splitting of longitudinal

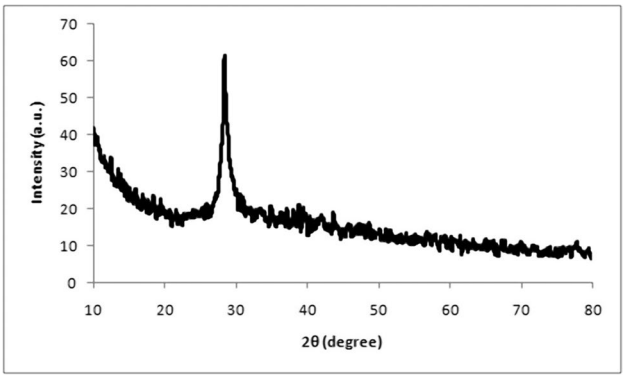


**Fig. 1** The XRD spectra of the sample F

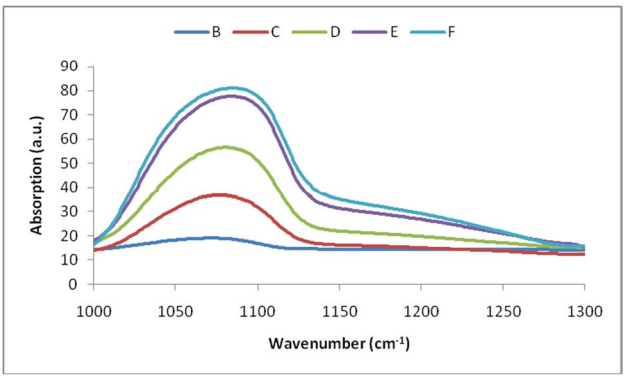


**Fig. 2** Infrared absorption spectra as a function of annealing temperature for the thermal treated samples

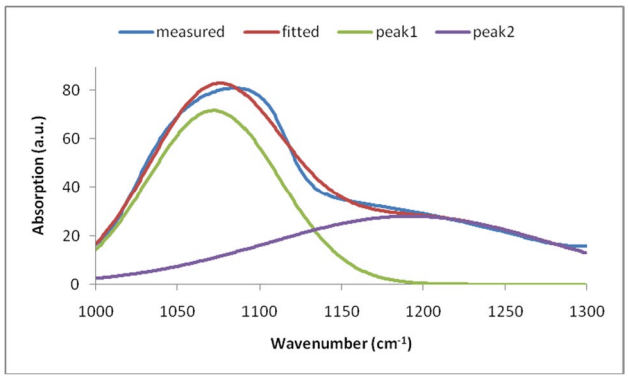


**Fig. 3** The deconvoluted (1000–1300) $cm^{-1}$ band in FTIR spectrum of the sample F

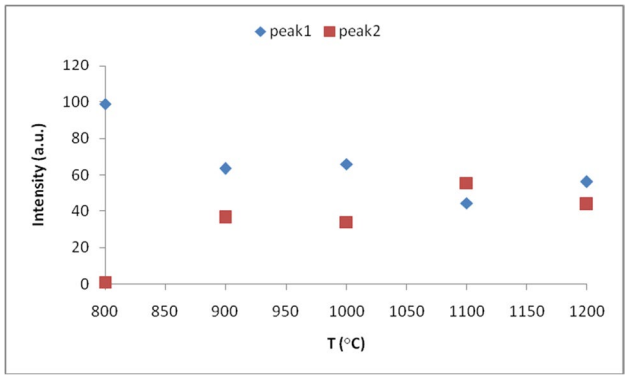


**Fig. 4** The intensities of the peaks 1 and 2 as function of annealing temperature

optical and transverse optical stretching motions [22]. The presence of this shoulder is an indication that each asymmetric broad peak noticed in the range 1000–1300 $cm^{-1}$ in FTIR spectra may be due to the overlapping of two peaks.

In order to investigate the overlapping peaks, each band in the region 1000–1300 cm-$^{1}$ was deconvoluted into two Gaussian–Lorentzian line shapes (peak1 and peak2). Figure 3 shows example of the deconvolution processes that concern the case of sample F that treated at 1200 $^{\circ}$C. The peak1 is attributed to asymmetric and symmetric stretching vibrations of Si–O-Si bonds and the $peak_2$ is due to the splitting of longitudinal optical and transverse optical stretching vibrations.

Figure 4 shows the intensities of the peaks 1 and 2 as functions of annealing temperature. We notice that, as the annealing temperature increases, the peak2 intensity increases at the expense of peak1 intensity with the tendency for the two peaks to have the same intensity at higher temperatures.

On the other hand, Fig. 5 shows that the ratio of the intensities of the two peaks (2:1) reaches its maxima at the

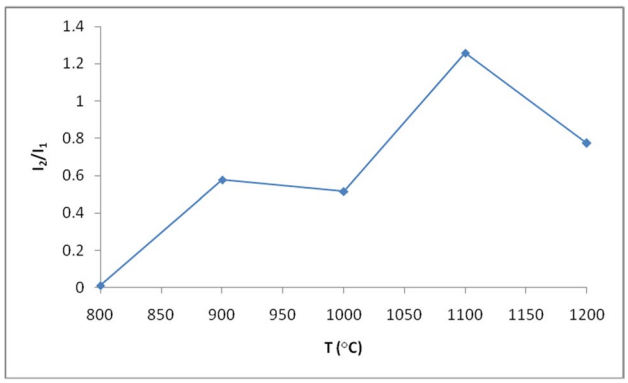


**Fig. 5** The ratio $I_2/I_1$ as a function of annealing temperature

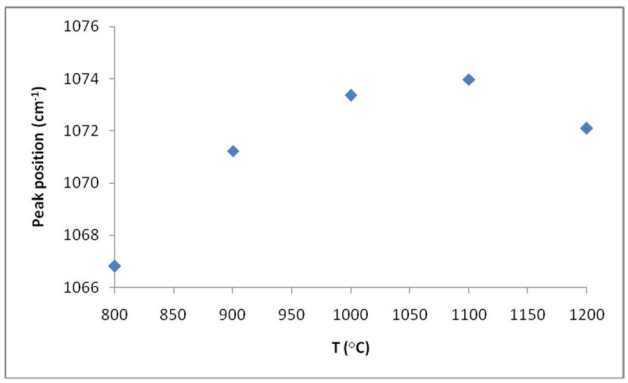


**Fig. 6** The peak1 position as a function of annealing temperature

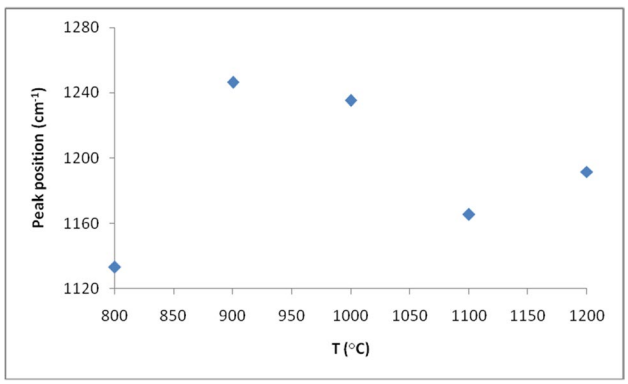


**Fig. 7** The peak2 position as a function of annealing temperature

annealing temperature 1100 $^{\circ}$C (sample E). In our previous work, we found that, at this annealing temperature the highest concentration of crystal defects is obtained. The decrease in the ratio value observed in the case of the sample annealed at 1200 $^{\circ}$C may be due to the regression of the splitting process.

Figures 6 and 7 show the position as a function of the annealing temperature for peaks 1 and 2. We notice that the

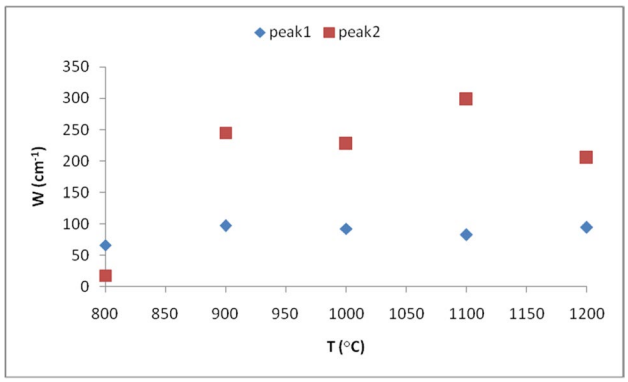


**Fig. 8** The peak width as a function annealing temperature

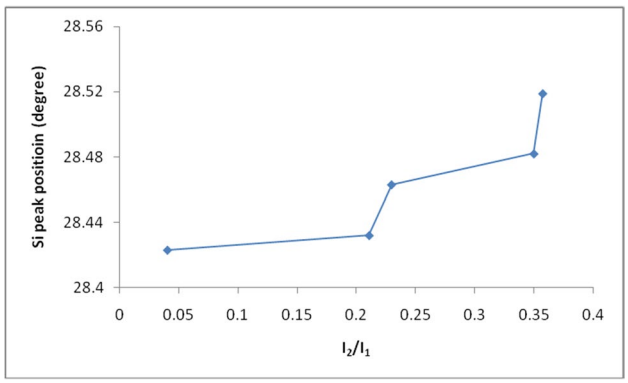


**Fig. 9** Silicon peak position as a function of the ratio $I_2/I_1$

position of peak2 is more affected by temperature than the position of peak1. In the case of $peak_1$ (Fig. 6), we notice that when the temperature increases within the range 800 – 1100 °C, the peak shifts towards the higher wave numbers. This behavior can be attributed to the changes in the structural composition of the surrounding environment because of silicon oxidation. However, the peak1 shifts back toward lower wavelengths upon annealing at T = 1200 °C (sample E). This is explained by the decrease in the intensity of the forces acting on the bonds because of the regression of the splitting process.

In the case of peak1 (Fig. 7), we notice that, when annealing at 900 °C, the shift towards higher wave numbers reaches its maximum due to the enhancement of the splitting process. As the temperature is raised above 900 °C, the peak shifts towards lower wave numbers due to the attractive forces to which the Si–O-Si bonds are exposed. Upon annealing at T = 1200 °C (sample E), the peak2 shifts back toward higher wavelengths due to the decrease in the intensity of the attractive forces because of the regression of the splitting process.

Figure 8 shows the peaks 1 and 2 width as functions of annealing temperature. It can be seen that while the width of peak1 does not appear to be significantly affected by the change in the annealing temperature, the width of peak2 is clearly affected by the changes in the structural composition of the surrounding environment imposed by the change in the oxidation temperature.

In our previous work [21], we found that thermal oxidation affects the intensity of the silicon peak in the XRD spectra. Here, we study the effect of oxidation on another parameter, the silicon peak position, by investigating the relationship between the ratio $I_2/I_1$ and the silicon XRD peak position (Fig. 9).

We notice that, as the ratio increases, the silicon peak shifts to the right and that the shift peaks in the case of sample F (annealed at 1200 °C). This result is evidence that peak2 growth causes defects in the silicon crystal structure.

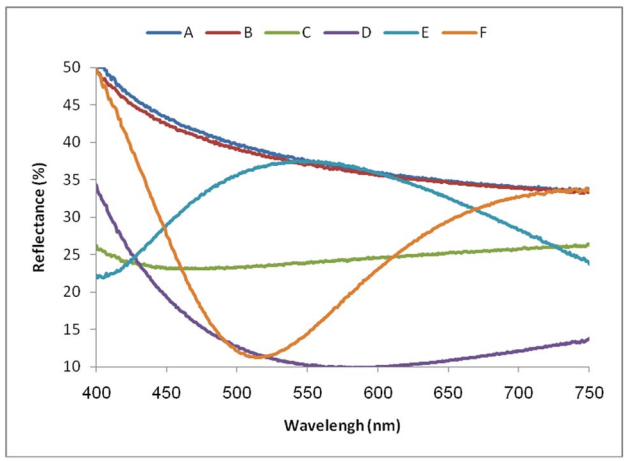


**Fig. 10** The reflectance spectra of the prepared samples in the range 400 – 750 nm

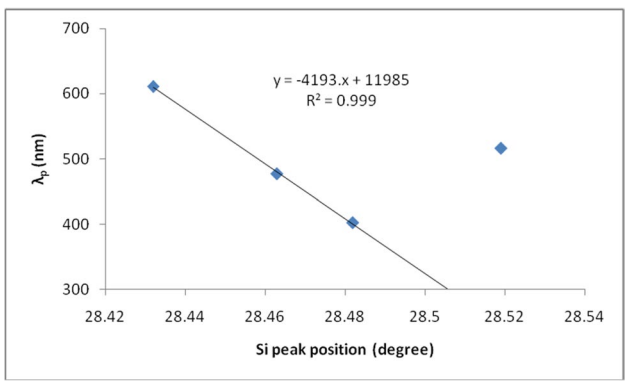


**Fig. 11** Plasma edge as a function of XRD Si peak position

This conclusion can be supported by optical reflectivity measurements, were in our previous work [21], we observed the formation of a plasma edge of silicon nanoparticles in the reflectivity spectra in the range 400–750 nm (Fig. 11). The plasma edge is not appearing in the spectra of the samples

Aand B. The formation of silicon nanoparticles is evidence of crystal defects [21] (Fig. 10).

Figure 11 illustrates the plasma edge as a function of the silicon XRD peak position.

We notice that, the plasma edge is proportional to the silicon peak position. The relationship between them is linear except for the point corresponding to the sample F at which the regression of the splitting process happened. This result supports the relationship between the peak shift and the formation of crystal defects, which we deduced from Fig. 9. This is because the shift of the plasma edge towards short wavelengths is associated with an increase in the concentration of conductive electrons [23, 24]. These electrons belong to silicon nanoparticles resulting from breaking the long-range arrangement of the silicon lattice as a result of the formation of crystal defects [22].

## 4 Conclusions

In this paper, pure n-type Silicon (111) wafers were thermal oxidized in air at different annealing temperatures (800 – 1200$^{\circ}$C). Annealing processes were performed using an oven. The effect of annealing temperature on XRD and FTIR spectra of the prepared samples was studied. The main results obtained in this study are:

- The thermal oxidation of silicon wafers at temperatures less than 1200 °C leads to enhance the phenomenon of the splitting of longitudinal optical and transverse optical stretching motions.
- The splitting phenomenon was verified by observing the appearance of two overlapping peaks in the region (1000–1300) $cm^{-1}$ in FT-IR spectra
- The splitting process leads to the formation of defects in the crystal structure of silicon, which in turn leads to the formation of silicon nanoparticles.

**Acknowledgements** The authors would like to thank the University of Damascus and the Higher Institute for Applied Sciences and Technology for providing the facility to carry out this research.

**Authors Contributions** Dr. Kamal characterized the samples and analyzed the results of the research, and was a major contributor in writing the manuscript. Miss Dalal performed the annealing procedures and contributed to the analysis of the results and the writing of the manuscript.

**Availability of Data and Materials** Not applicable.

## Declarations

**Consent with Ethical Standards** This is an observational study. No ethical approval is required.

**Consent to Participate** Not applicable.

**Consent for Publication** Not applicable.

**Conflict of Interests** Not applicable.

## References

1. Feldmann F, Bivour M, Reichel C, Steinkemper H, Hermle M, Glunz SW (2014) Tunnel oxide passivated contacts as an alternative to partial rear contacts. Sol Energy Mater Sol Cells 131:46–50
2. Moldovan A, Feldmann F, ZimmerM RJ, Benick J, Hermle M (2015) Tunnel oxide passivated carrier-selective contacts based on ultra-thin SiO2 layers. Sol Energy Mater Sol Cells 142:123–127
3. Muhtazaruddin N, Amran M (2019) Thermal oxidation improvement in semiconductor wafer fabrication. J Power Electron Drive Syst 10:1141–1147
4. Bian JY, Zhang LP, Guo WW, Wang DL, Meng FY, Liu ZX (2014) Improved passivation effect at the amorphous/crystalline silicon interface due to ultrathin SiOx layers pre-formed in chemical solutions. APEX 7:065504
5. Seif JP, Descoeudres A, Filipiè M, Smole F, Topiè M, Charles Holman Z, De Wolf S, Ballif C (2014) Amorphous silicon oxide window layers for high-efficiency silicon heterojunction solar cells. J Appl Phys 115:024502
6. Ohdaira K, Oikawa T, Higashimine K, Matsumura H (2016) Suppression of the epitaxial growth of Si films in Si heterojunction solar cells by the formation of ultra-thin oxide layers. Curr Appl Phys 16:1026–1029
7. Rölver R, Berghoff B, Bätzner D, Spangenberg B, KurzH SM, Stegemann B (2008) Si/SiO2 multiple quantum wells for all silicon tandem cells: conductivity and photocurrent measurements. Thin Solid Films 516:6763–6766
8. Stegemann B, Schoepke A, Schmidt M (2008) Structure and photoelectrical properties of SiO2/Si/SiO2 single quantum wells prepared under ultrahigh vacuum conditions. J Non-Cryst Solids 354:2100–2104
9. Gallet J, Silly G, El Kazzi M, Bournel F, Sirotti F, Roche F (2017) Chemical and kinetic insights into the thermal decomposition of an oxide layer on Si(111) from millisecond photoelectron spectroscopy. Sci Rep 7:14257
10. Himpsel FJ, McFeely FR, Taleb-Ibrahimi A, Yarmoff JA, Hollinger G (1988) Microscopic structure of the SiO2/Si interface. Phys Rev B 38:6084–6096
11. Hirose K, Nohira H, Azuma K, Hattori T (2007) Photoelectron spectroscopy studies of SiO2/Si interfaces. Progr Surf Sci 82:3–54
12. Sieger MT, Luh DA, Miller T, Chiang TC (1996) Photoemission extended fine structure study of the SiO_{2}/Si(111) interface. Phys Rev Lett 77:2758–2761
13. Luh DA, Miller T, Chiang TC (1997) Statistical cross-linking at the Si(111)/SiO_{2} interface. Phys Rev Lett 79:3014–3017
14. Brower KL (1988) Kinetics of H2 passivation of Pb centers at the (111) Si-SiO2 interface. Phys Rev B 38:9657–9666
15. Deal BE, Grove AS (1965) General relationship for the thermal oxidation of silicon. J Appl Phys 36:3770–3778
16. Hattori T (1995) Chemical structures of the SiO2Si interface. Crit Rev Solid State Mater Sci 20:339–382
17. Starodub D, Gusev EP, Garfunkel E, Gustafsson T (1999) Silicon oxide decomposition and desorption during the thermal oxidation of silicon. Surf Rev Lett 6:45–52
18. 1998 Fundamental Aspects of Ultrathin Dielectrics on Si-Based Devices. Garfunkel E, Gusev E, Vul A (eds). Kluwer, Dordrecht/Boston/London

19. IshizakaA ShirakiY (1986) Low temperature surface cleaning of silicon and its application to silicon MBE, 671. J Electrochem Soc 133:666
20. Daldosso N, Das G, Larcheri S, Mariotto G, Dalba G, Pavesi L, Irrera A, Priolo F, Iacona F, Rocca F (2007) Silicon nanocrystal formation in annealed silicon-rich silicon oxide films prepared by plasma enhanced chemical vapor deposition. J Appl Phys 101:113510
21. Kayed K, Kurd DB (2021) The effect of annealing temperature on the structural and optical properties of $Si/SiO_2$ composites synthesized by thermal oxidation of silicon wafers. Silicon. https://doi.org/10.1007/s12633-021-01307-w
22. Lange P, Windbracke W (1989) Characterization of thermal and deposited thin oxide layers by longitudinal optical-transverse optical excitation in fourier transform IR transmission measurements. Thin Solid Films 174:159–164
23. Kayed K, Alberni LL (2020) The effect of annealing temperature on the plasma edge in reflectance spectra of $Al/Al_2O_3$ composites synthesized by thermal oxidation of aluminum thin films. Plasmonics 15:1959–1966
24. Kayed K, Alberni LL (2021) Effect of thermal oxidation on the structural and optical properties of aluminum thin films prepared by DCMagnetron sputtering**.** Poster presented at Damascus University - Workshop for Scientific Research. https://doi.org/10.13140/RG.2.2.33219.73765.